



Co-assembly of a Nafion–Mesoporous Zirconium Phosphate Composite Membrane for PEM Fuel Cells

A. K. Sahu¹, S. Pitchumani¹, P. Sridhar¹, and A. K. Shukla^{1,2,*}

¹ Central Electrochemical Research Institute, Karaikudi-630 006, India

² Solid State and Structural Chemistry Unit, Indian Institute of Science, Bangalore-560 012, India

Received February 3, 2009; accepted March 4, 2009

Abstract

Synthesis of mesoporous zirconium phosphate (MZP) by co-assembly of a tri-block copolymer, namely pluronic-F127, as a structure-directing agent, and a mixture of zirconium butoxide and phosphorous trichloride as inorganic precursors is reported. MZP with a specific surface area of $84 \text{ m}^2 \text{ g}^{-1}$, average pore diameter of about 17 nm and pore volume of $0.35 \text{ cm}^3 \text{ g}^{-1}$ has been prepared, and characterised by X-ray diffraction (XRD) and transmission electron microscopy. Nafion–MZP composite membrane is obtained by employing MZP as a surface-functionalised solid-super-acid-proton-conducting medium as well as an inorganic filler with high affinity to absorb water and fast proton-transport across the electrolyte membrane even under low relative humidity (RH) conditions. The composite membranes have been evaluated in H_2/O_2 polymer electrolyte fuel cells

(PEFCs) at varying RH values between 18 and 100%; a peak power density of 355 mW cm^{-2} at a load current density of $1,100 \text{ mA cm}^{-2}$ is achieved with the PEFC employing Nafion–MZP composite membrane while operating at optimum temperature ($70 \text{ }^\circ\text{C}$) under 18% RH and ambient pressure. On operating the PEFC employing Nafion–MZP membrane electrolyte with hydrogen and air feeds at ambient pressure and a RH value of 18%, a peak power density of 285 mW cm^{-2} at the optimum temperature ($60 \text{ }^\circ\text{C}$) is achieved. In contrast, operating under identical conditions, a peak power density of only $\sim 170 \text{ mW cm}^{-2}$ is achieved with the PEFC employing Nafion-1135 membrane electrolyte.

Keywords: Co-assembly, Composite Membrane, Mesoporous Zirconium Phosphate, PEFC, Relative Humidity

1 Introduction

Among the competing fuel cell technologies, polymer electrolyte fuel cells (PEFCs) are commercially most attractive owing to their quick start-up and ambient-temperature operations. PEFCs can also deliver operational efficiencies as high as 64% with both specific and volumetric energy densities comparable to internal combustion engines while emitting no pollutants [1]. However, PEFCs consume about 20% of the generated power in supporting its auxiliary units [1]. One of the ways to reduce the auxiliary power demand of the PEFCs is to employ electrolyte membranes that could operate under low relative humidity (RH) conditions making the system simpler and hence cost-effective. Accordingly, efforts have been expended to produce suitably modified Nafion-composite membranes with ceramic/inorganic fillers such as SiO_2 , TiO_2 , ZrO_2 and zeolites [2–13]. The addition of inorganic fillers narrows the hydrophilic channels in Nafion®

matrix from 7.9 to 6.5 nm, facilitating proton conduction [14]. Besides, the filler particles have affinity to absorb and retain water in the Nafion matrix keeping it adequate for proton conduction.

Zirconium phosphate as a hydrophilic and proton conducting material has been incorporated into various polymer matrices [15–28]. It is noteworthy that proton conduction in these polymers predominantly takes place by surface transport through the interlayer regions in the presence of water. In the literature, Nafion–zirconium phosphate composite membranes have been fabricated by a variety of techniques [15, 29–33]. Conventionally, water absorbing pre-formed fine zirconia powder is dispersed in the Nafion ionomer solution to form Nafion–zirconia composite membrane. The compos-

[*] Corresponding author, akshukla2006@gmail.com

ite membrane is then treated in phosphoric acid followed by drying at suitable temperature for forming Nafion–zirconium phosphate composite membrane. Another method includes the cation exchange between the ionomer and zirconium cationic species followed by membrane treatment with phosphoric acid in order to precipitate zirconium phosphate within the hydrophilic regions of the ionomer. In an *in situ* preparation of the zirconium phosphate, phosphoric acid is reacted with either zirconyl chloride or with zirconium alkoxide at desired temperatures; zirconium phosphate, thus prepared, is embedded within Nafion ionomer to form a composite membrane. Incorporating the zirconium phosphate into the polymeric matrix by the aforesaid processes could result in a non-homogeneous matrix with such fillers; besides phosphoric acid may not be covalently bound within the membrane. It is also possible to end up with enriched concentrations of the phosphoric acid on the surface of the composite membrane and when operated in the PEFC may cause its leaching along with the product water. Among the various aforesaid techniques for preparing Nafion–zirconium phosphate composite membranes, only the *in situ* preparation of zirconium phosphate for embedding with Nafion ionomer to form a composite membrane appears appropriate to avoid the presence of any surface bound acid. However, even in this preparation, both low porosity and low internal-surface areas of zirconium phosphate limit the hydrophilicity of the composite membrane. In order to increase the porous nature of zirconium phosphate, efforts are being expended to develop mesoporous zirconium phosphate (MZP) materials by either hard template approach or by surfactant-assisted route [35–43]. MZP as a surface-functionalised solid-superacid-proton-conducting medium as well as an inorganic filler with high affinity to absorb water helps fast proton transport across the electrolyte membrane suitable for PEFC operation especially at low RH values.

In this communication, a novel method to synthesise MZP using a structure-directing cationic surfactant by a co-assembly route is reported where the presence of large pores and high internal-surface-area ameliorates the hydrophilic character. MZP, thus synthesised, is impregnated with the Nafion ionomer to fructify a proton-conducting composite membrane. The performances of PEFCs employing these composite membranes at RH values between 18 and 100% are superior to PEFCs with pristine Nafion membranes operating under identical conditions.

2 Experimental Details

MZP was synthesised by a co-assembly route similar to the process reported by Tian et al. [44]. In brief, 1.4 g of surfactant, Pluronic-F127 (Aldrich) was dissolved in absolute ethanol (Merck, Germany). Subsequently, 0.69 g of phosphorus trichloride (Merck, Germany) was added dropwise to the solution with continuous stirring for another 30 min. To

this, 2.33 g of zirconium butoxide (Aldrich) diluted with ethanol in the presence of HCl as a catalyst was added. The solution was stirred for another 1 h and left over a week for gelation. The gel was cured at 80 °C for 24 h and calcined at 500 °C for 5 h in a programmed muffle furnace heated from 30 to 200 °C at 1 °C min⁻¹ and from 200 to 550 °C at 3 °C min⁻¹. During the heat treatment, the surfactant was removed while maintaining the acidity and amorphous characteristics of the material. The resultant material was collected and ground to fine powder. The required amount of MZP was then impregnated with 5% commercial Nafion solution (DuPont) and the resultant admixture was ultra-sonicated for 30 min followed by mechanical stirring for 12 h. The admixture was then transferred to a flat Plexiglass plate and allowed to dry overnight at 80 °C in a vacuum oven. The composite membrane thus formed was detached by adding water. The thickness of the finished membrane was ~ 90 μm.

XRD patterns of MZP materials at small angles ($2\theta = 0.1\text{--}10^\circ$) were recorded using a Bruker AXS D8 Advance Diffractometer in $\theta\text{--}\theta$ configuration using CuK_α radiation. Textural and surface properties of MZP were characterised by N_2 physisorption and temperature-programmed desorption, respectively. Nitrogen adsorption–desorption isotherms were measured at 77 K using a Micromeritics ASAP 2020. Total surface area and pore volumes were determined using the Brunauer–Emmett–Teller (BET) equation and the single-point method, respectively. Pore-size distribution (PSD) curves were obtained by Barrett–Joyner–Halenda (BJH) method and the position of the maximum of the PSD was used as the average pore diameter. MZP was also examined under a 200 kV Tecnai-20 G2 transmission electron microscope (TEM) for determining pore size. For these measurements, the sample was suspended in acetone with ultrasonic dispersion for 3 min. Subsequently, a drop of this suspension was deposited on a holey carbon grid and allowed to dry. Images were recorded with a MultiScan CCD Camera (model 794 Gatan) using low-dose conditions. The presence and distribution of MZP particles in the composite membrane were ascertained with the help of a HITACHI S-3000H scanning electron microscope (SEM) coupled with electron dispersive analysis by X-rays (EDAX) facility.

Proton conductivity measurements were performed on the membrane in a typical two-electrode cell by ac impedance technique. The conductivity cell comprised two stainless steel electrodes, each of 20 mm diameters. The membrane sample was sandwiched between the two stainless steel electrodes fixed in a Teflon block and kept in a closed glass container. Desired RH values in the test chamber were maintained using salt solutions as described in ref. [45]. AC impedance spectra of the membrane were recorded in the frequency range between 1 MHz and 10 Hz with 10 mV amplitude using an Autolab PGSTAT 30. The resistance value (within experimental error of $\pm 3\%$) associated with the membrane conductivity was determined from the high-frequency intercept of the impedance with the real axis. The membrane conductivity

was calculated from the membrane resistance, R , using the equation:

$$\sigma = \frac{l}{RA} \quad (1)$$

where σ is the proton conductivity of membrane (S cm^{-1}), l the membrane thickness (in cm) and A is the cross-sectional area of the membrane samples (in cm^2).

PEFCs comprising Nafion–MZP composite membranes were performance tested at varying RH values between 18 and 100% while feeding with H_2/O_2 and H_2/air at atmospheric pressure and the results were compared with the PEFC comprising commercial Nafion-1135 membrane operating under identical conditions. For making membrane electrode assemblies (MEAs), diffusion-layer coated carbon papers (SGL, thickness = 0.27 mm) were used as backing layers. For the catalyst layer, 40 wt.-% Pt/C (Johnson Matthey) was dispersed in a mixture of 2-propanol and Nafion solution followed by ultrasonication for 20 min to form a homogeneous slurry that was applied onto the diffusion layer. The catalyst loadings on both the anode and the cathode (active area: 25 cm^2) were kept at 0.5 mg cm^{-2} . A thin layer of Nafion ionomer was applied to the catalyst surface of both the electrodes and MEAs were obtained by hot pressing the Nafion-1135 membrane sandwiched between cathode and anode under 15 kN ($\sim 60 \text{ kg cm}^{-2}$) at $125 \text{ }^\circ\text{C}$ for 3 min; in a similar manner, the MEAs with Nafion–MZP composite membranes were obtained. These MEAs were performance tested at varying RH values between 18 and 100% at atmospheric pressure in a conventional 25 cm^2 PEFC fixture with parallel-serpentine flow field machined on graphite plates.

The PEFC was maintained at ca.100% RH by passing hot and wet hydrogen and oxygen gases to its anode and cathode sides, respectively, at a flow rate of 1 L min^{-1} through a mass-flow controller. The RH of the PEFC depends on the mass of water vapour (D), saturated vapor[®] pressure of water (P_{sat}) and moisture content (mH_2O). In order to operate the PEFC at varying RH values between 18 and 100%, parameters such as dew-point temperature (DPT), gas temperature (GT)/gas-supply temperature (GST) and dew-point-humidification temperature (DPHT) were adjusted using an Arbin Fuel Cell Test Station (Model PEM-FCTS-158541) procured from Arbin Instruments (US) as described in ref. [7]. After establishing and equilibrating the desired humidity level, the polarisation data on the PEFCs were collected. The reproducibility of the data was ascertained by repeating the experiments at least twice.

3 Results and Discussion

XRD pattern (Figure 1) for the calcined MZP shows a broad diffraction peak at $2\theta = 0.7^\circ$, indicative for the presence of randomly ordered mesostructures [46]. N_2 adsorption–desorption isotherms for synthesised MZP powders and their corresponding pore-size distributions (PSDs) are shown in Figure 2 and 3, respectively. According to IUPAC classifica-

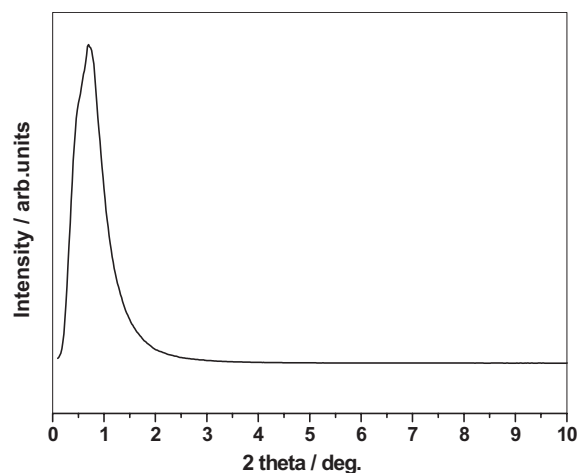


Fig. 1 Powder XRD pattern for MZP powder.

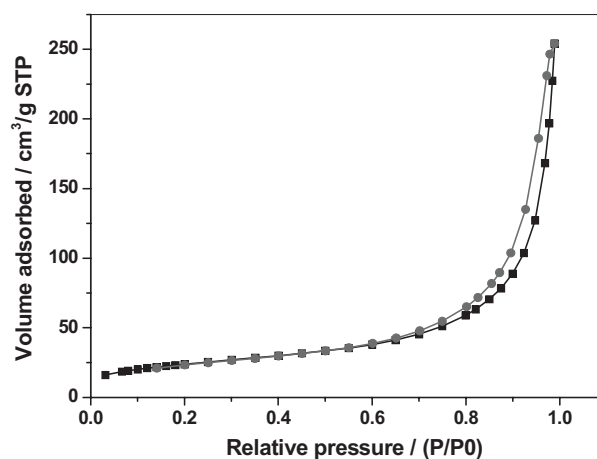


Fig. 2 N_2 adsorption–desorption isotherm for MZP powder.

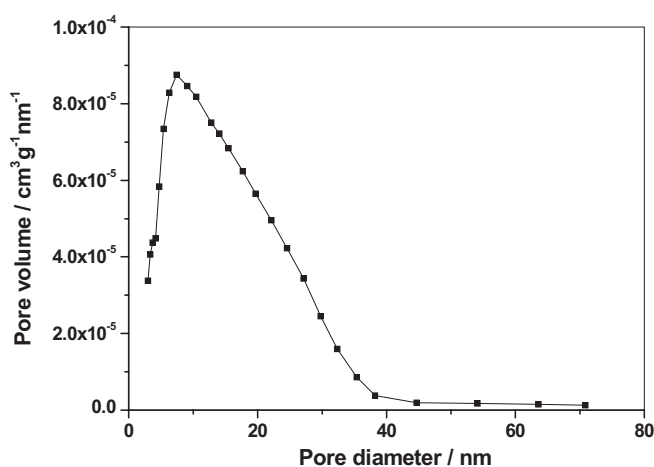


Fig. 3 Pore-size distribution for MZP powder.

tion, N_2 adsorption–desorption isotherms for this material are of type I/II and the hysteresis loop belongs to type H3 indicating the presence of relatively large pores, while type II isotherm is typically observed for non-porous and macro-por-

ous materials. The specific surface area for synthesised MZP is found to be $84 \text{ m}^2 \text{ g}^{-1}$ [11]. The pore volume of synthesised MZP is $0.35 \text{ cm}^3 \text{ g}^{-1}$. The PSD analysis derived from the adsorption branch of the isotherms through the BJH method indicates the presence of pores with wide diameters of around 17 nm. Figure 4 shows the TEM image of MZP powder where irregular porous structure of the materials is clearly visible. It is noteworthy that the absence of long-range pore ordering is achieved, without any hard-template approach during the synthesis of MZP, but by the mere use of pluronic-F127 as a mild structure-directing agent.

The aforesaid data establish the mesoporous nature of zirconium phosphate material. These data are seminal for fabricating Nafion–MZP composite membranes of required thickness. SEM micrograph in Figure 5 shows a crack-free membrane with uniform distribution of the filler particles. The presence of spherical-shaped nanopores in the filler particles is also visible. Quantitative elemental analysis data for Nafion–MZP composite membrane obtained from electron dispersive analysis by X-ray (EDAX) are presented in Table 1.

Large pores and high internal-surface area for MZP make its internal pore surfaces hydrophilic and facilitate proton conduction. This is not generally observed when highly crystalline zirconia powder is incorporated with Nafion solution for realising a composite membrane followed by its soaking in phosphoric acid. Such a composite membrane is found to be prone to phosphoric acid leaching by water generated during the PEFC operation. The Nafion–MZP composite membrane reported here is formed by a single-step sol–gel route and hence mitigates the aforesaid problem. Figure 6 shows a plot of proton conductivity of pristine Nafion and Nafion–MZP composite membranes as a function of RH. The proton

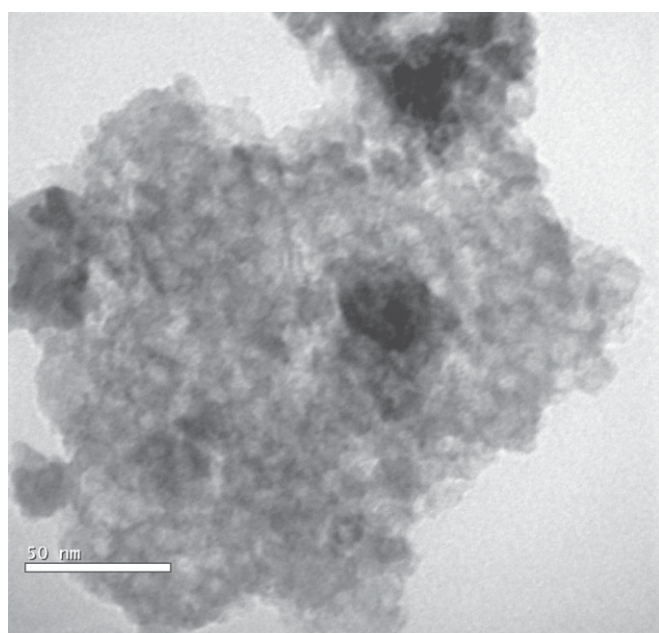


Fig. 4 TEM images for MZP powder.

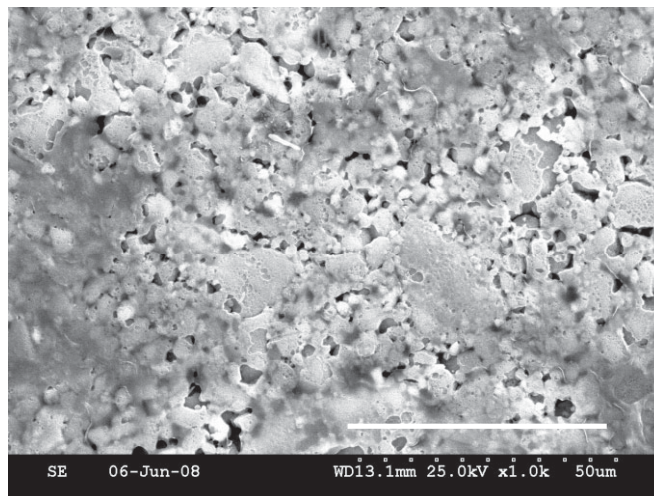


Fig. 5 Typical SEM photographs for Nafion–MZP composite membrane. The scale bar is 50 μm .

Table 1 Quantitative EDAX data for Nafion–MZP (5 wt.-%) composite membrane.

Element	Net Counts	ZAF	Weight%	Atom%	Formula
C	268	6.812	12.58	21.54	C
O	2,665	5.326	19.66	25.28	O
F	5,599	5.789	37.19	40.26	F
P	20,832	1.400	12.91	8.58	P
S	1,031	1.766	0.89	0.57	S
S	0	0.000	–	–	
Zr	1,435	0.000	–	–	
Zr	21,960	1.227	16.77	3.78	Zr
Zr	0	0.000	–	–	
Total			100.00	100.00	

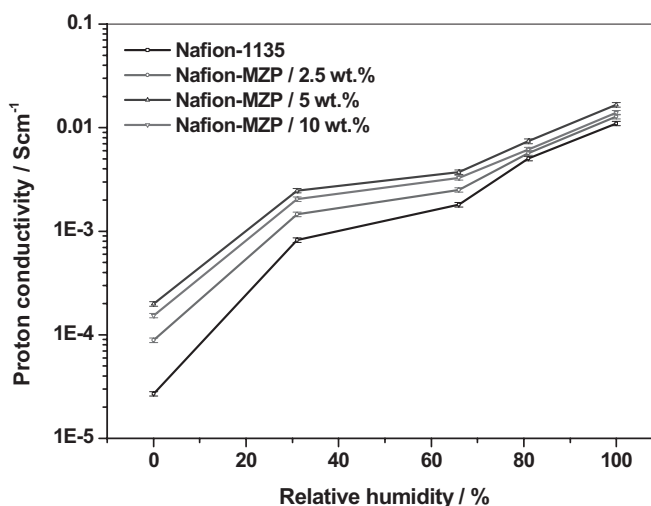


Fig. 6 Variation in proton conductivity for Nafion-1135 and Nafion–MZP composite membranes as a function of RH.

conductivity of the pristine Nafion membrane under fully humidified condition is $1.1 \times 10^{-2} \text{ S cm}^{-1}$ at 30 °C. The proton conductivity of Nafion membrane decreases as the RH value decreases; at 0% RH, the conductivity of the Nafion mem-

brane is found to be only $2.75 \times 10^{-5} \text{ S cm}^{-1}$. The proton conductivity of the Nafion–MZP composite membranes is higher in relation to pristine Nafion membrane at all RH values. Under fully humidified condition (ca. 100% RH), a maximum proton conductivity of $1.66 \times 10^{-2} \text{ S cm}^{-1}$ is exhibited by Nafion–MZP (5 wt.-%) composite membrane. The decrease in the proton conductivity of Nafion–MZP (10 wt.-%) composite membranes may be due to the presence of excess filler that hinders the proton conduction path in the Nafion matrix. Similar to the pristine Nafion membrane, the proton conductivity of Nafion–MZP composite membranes decreases with RH. However, the conductivity of the composite membranes happens to be higher than the pristine Nafion membrane at all RH values. It is noteworthy that at 30% RH, the conductivity of Nafion–MZP (5 wt.-%) composite membrane is about one order of magnitude higher than the corresponding conductivity values for pristine Nafion membrane. At lower RH values, desorption of water molecules on sulphonic acid sites in Nafion leads to reduced proton mobilities, and channel pinch-off that results in lack of formation of properly ordered microphase separation lowering its overall proton conductivity. By contrast, Nafion–MZP composite membranes have enhanced water-holding capacity due to stronger absorption of water on the interior pore surfaces that help retaining its proton conductivity.

Performance evaluation for H_2/O_2 PEFCs employing Nafion–MZP composite membranes has been conducted by obtaining respective polarisation curves at varying RH values between 18 and 100% under ambient pressure. During all the experiments, the flow rates for both the fuel and the oxidant are kept at 1 L min^{-1} . Figure 7 shows the polarisation curves for Nafion–MZP composite membranes and commercial Nafion-1135 membrane under $\sim 100\%$ RH at 70°C . PEFCs containing Nafion–MZP composite membranes with varying MZP contents show better performance than the PEFC with pristine Nafion membrane. Maximum proton conductivity with composite membrane is attained at an intermediate

loading of MZP. The data reflect the resistance values for the PEFCs with Nafion–MZP composite membrane to be lower than the PEFC with Nafion membrane; the resistance being lowest for the PEFC with 5 wt.-% Nafion–MZP composite membrane. The peak power density of 725 mW cm^{-2} is achieved for the PEFC with Nafion–MZP (5 wt.-%) composite membrane in relation to 655 mW cm^{-2} for the PEFC with Nafion-1135 membrane operating under identical conditions. It is obvious that the existence of MZP as a surface functionalised solid super-acid proton conducting medium in the Nafion matrix assists Nafion–MZP composite membrane to achieve higher proton conductivity in relation to pristine Nafion membrane. Proton conductivity in the composite membrane is attributed to protons transferred through hydrogen bonding with water-filled ion pores. However, an excess of MZP could inhibit proton conduction in the membrane, disrupting the continuity of proton conduction paths in the Nafion membrane [7]. Accordingly, peak power density for the PEFC with the Nafion–(10 wt.-%) MZP composite membrane is slightly lower than the PEFC employing Nafion–(5 wt.-%) MZP composite membrane.

Polarisation curves for PEFCs with Nafion–MZP composite and commercial Nafion-1135 membranes at 50% RH are presented in Figure 8. It is seen that the performances for all the PEFCs are lower in relation to the PEFCs with fully humidified Nafion–MZP electrolyte membranes as shown in Figure 7. However, from the data in Figure 8, it is observed that the performance of PEFCs with Nafion–MZP composite membranes is superior to PEFCs with pristine Nafion membrane. A maximum peak power density of 581 mW cm^{-2} is achieved for Nafion–MZP (5 wt.-%) composite membrane compared to 502 mW cm^{-2} for commercial Nafion-1135 membrane. This elucidates that MZP helps water retention in the Nafion–MZP composite membrane and keeps the membrane adequately hydrated. Polarisation curves for PEFCs with Nafion–MZP composite membrane and Nafion-1135 at 31% RH values are presented in Figure 9. It is seen from the data

that the PEFCs with pristine Nafion membrane exhibit poor performance in relation to the PEFCs with Nafion–MZP composite membranes, as the former could easily lose water from its framework. The peak power density obtained for PEFCs with Nafion-1135 is around 268 mW cm^{-2} . In contrast, PEFC performance improves with increased MZP content in the Nafion–MZP composite membrane and attains a maximum at MZP content of 5 wt.-% as shown in Figure 9. A peak power density of 455 mW cm^{-2} is achieved at this RH value for PEFCs with Nafion–MZP composite membranes. The polarisation curves for PEFCs with Nafion-1135 and Nafion–MZP composite membranes under near-dry condition ($\sim 18\%$ RH) are shown in Figure 10. At this RH value, PEFCs with pristine Nafion-1135 membranes yield a peak power density of only about 224 mW cm^{-2} at the load current density value of 500 mA cm^{-2} , primarily due to the

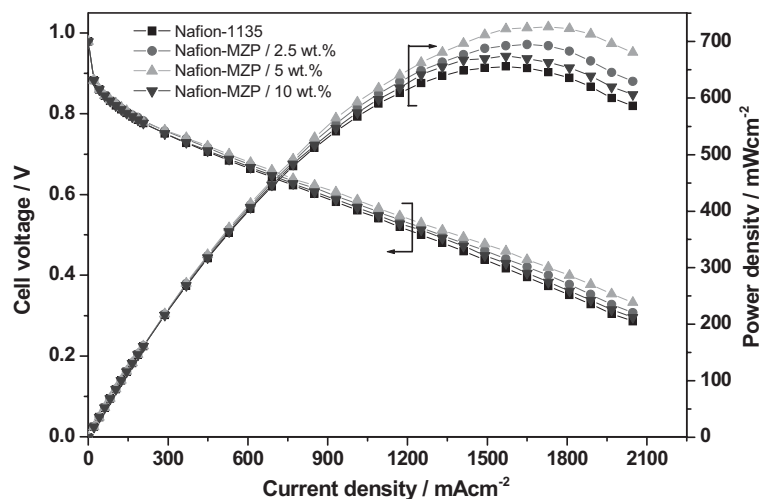


Fig. 7 Performance of a H_2/O_2 PEFC employing Nafion-1135 and Nafion–MZP composite membranes at 100% RH at 70°C under atmospheric pressure.

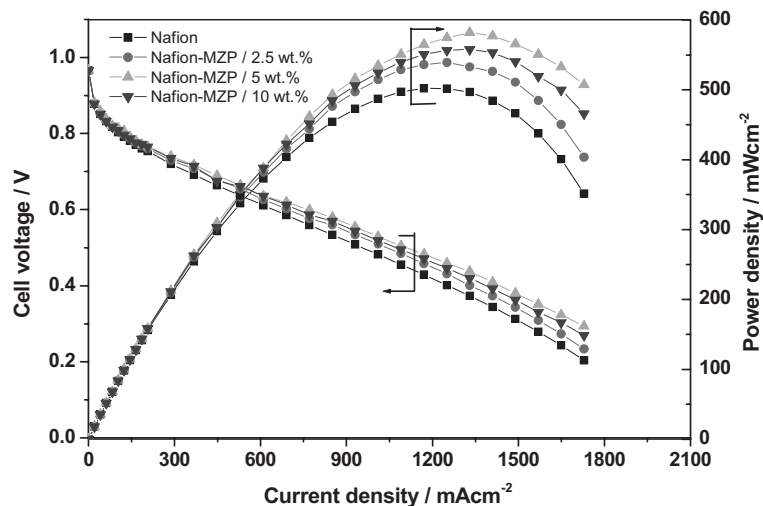


Fig. 8 Performance of a H_2/O_2 PEFC employing Nafion-1135 and Nafion-MZP composite membranes at 50% RH at 70 °C under atmospheric pressure.

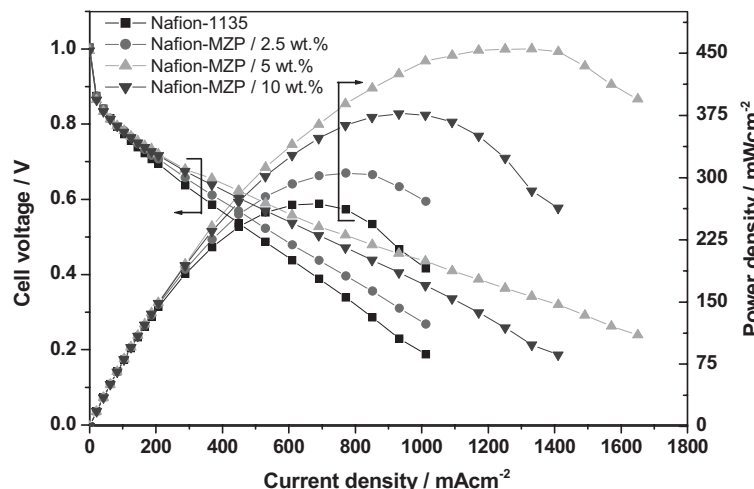


Fig. 9 Performance of a H_2/O_2 PEFC employing Nafion-1135 and Nafion-MZP composite membranes at 31% RH at 70 °C under atmospheric pressure.

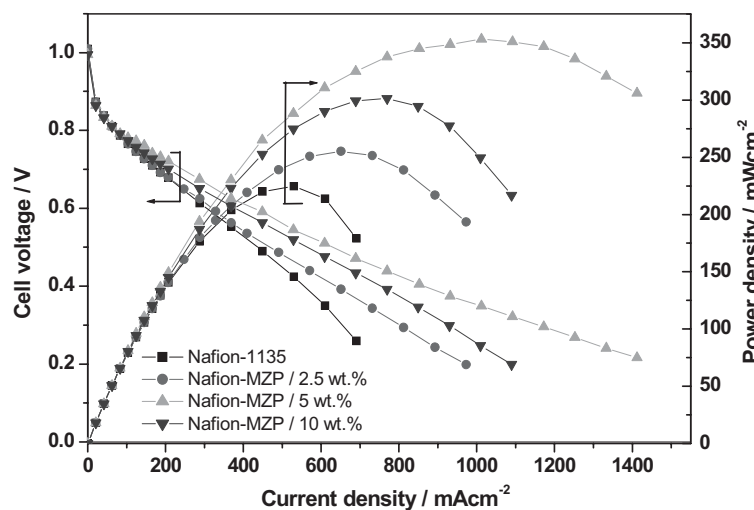


Fig. 10 Performance of a H_2/O_2 PEFC employing Nafion-1135 and Nafion-MZP composite membranes at 18% RH at 70 °C under atmospheric pressure.

poor conductivity of the Nafion membrane. In contrast, under identical conditions, PEFCs employing Nafion–MZP composite membranes perform much better. The performance of PEFCs with Nafion–MZP composite membranes increases gradually with increase in MZP content in the Nafion matrix. A peak power density of 353 mW cm^{-2} is achieved at a load current density value of $1,100 \text{ mA cm}^{-2}$ for the PEFC employing a Nafion–MZP composite membrane with 5 wt.-% MZP while operating at 70 °C under atmospheric pressure.

PEFCs employing Nafion-1135 membrane and Nafion–(5 wt.-%) MZP composite membranes have also been performance tested in air with varying RH values and the data are presented in Figure 11. The performance of the PEFC employing Nafion–MZP composite membrane is superior in relation to the PEFC employing pristine Nafion membrane at all RH values while operating at 60 °C under atmospheric pressure. It is noteworthy that at 18% RH value, a peak power density of 285 mW cm^{-2} at a load current density value of 800 mA cm^{-2} is achieved with Nafion–MZP composite membrane in contrast to the peak power density of only 170 mW cm^{-2} at a load current density value of 500 mA cm^{-2} achievable with the PEFC employing pristine Nafion membrane operating under identical conditions.

The area-specific resistance (R) for PEFCs employing Nafion and Nafion–MZP composite membranes under varying RH values is measured and the data are presented in Table 2. PEFCs employing Nafion–MZP composite membranes exhibit lower area-specific resistance in relation to the PEFC employing pristine Nafion-1135 membrane and the effect is clearly seen at low RH values; the increase in resistance at low RH values being significantly higher for pristine Nafion membrane in relation to the Nafion–MZP composite membrane. This is a clear manifestation of the ability of MZP in reducing membrane resistance due to its water retention property.

From the foregoing, it is obvious that PEFC performance is closely related to the water management issue. In commercial Nafion membranes, due to the limited availability of water at the anode, electro-osmotic drag of water from anode to cathode and insufficient water diffusion from cathode to anode affect the MEA to dehydrate. The membrane dehydration is manifested with an increase in the ohmic resistance of the cell, leading to decreased cell performance. In contrast, in the case of composite Nafion membranes such a problem is obviated.

It is noteworthy that the positively charged zirconia particles counterbalance the negatively charged sulphonate groups present in Nafion enhancing its

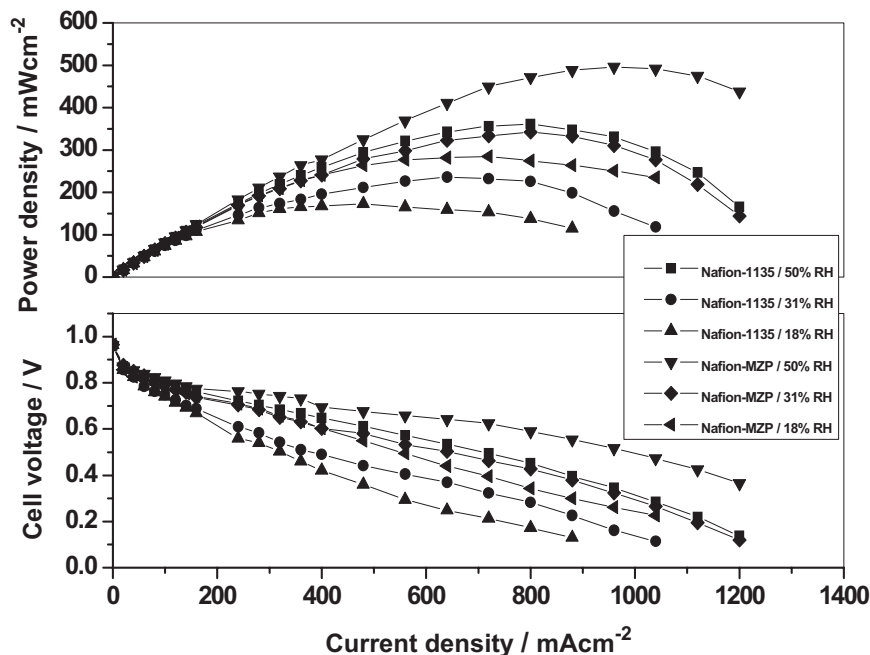


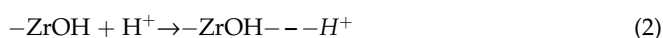
Fig. 11 Performances of H₂/air PEFCs employing Nafion-1135 and Nafion-(5 wt.-%) MZP composite membranes with varying RH values at 60 °C under atmospheric pressure.

Table 2 Area specific resistance data for PEFCs employing Nafion and Nafion–MZP composite membranes at varying RH values.

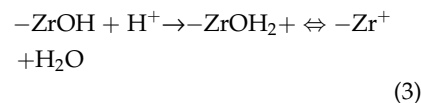
Membrane	Area specific resistance (R) in (Ω cm ²) at varying RH values			
	100% RH	50% RH	31% RH	18% RH
Nafion–1135	0.255	0.324	0.648	0.776
Nafion–MZP (2.5 wt.-%)	0.242	0.304	0.568	0.692
Nafion–MZP (5 wt.-%)	0.232	0.285	0.375	0.514
Nafion–MZP (10 wt.-%)	0.245	0.293	0.431	0.561

hydrophilic character. The long-range coulombic attractive forces between protons and sulphonate groups are disrupted by the presence of positively charged zirconia particles in the membrane, facilitating the protons to readily pass through the membrane pores. Hence, the proton conductivity of the membrane is maintained, but is lower than the corresponding proton-conductivity values at high RH.

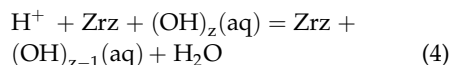
Enhanced proton conduction at low RH values in the Nafion–MZP composite membranes reported in this study could be visualised in the light of the following discussion. Upon exposure to water, anhydrous zirconia, which has an isoelectric point, i.e. the pH at which the particles carry zero charge, of 2 is hydrated primarily in two ways: (i) physical adsorption of water molecules, including hydrogen bonding to surface oxygen ions without any dissociation, and (ii) chemisorption of water with dissociation resulting in surface–ZrOH groups. The physical adsorption is represented by



while chemisorption is represented by



Equation [3] is analogous to



During the cell operation, protons are continuously generated at the anode and are driven across the membrane, but the sulphonate groups remain largely unprotonated, even at low pH values. In the absence of essentially immobile counter cations in the pore fluid, this would retard the free migration of protons through the membrane, whereas the hydrophilic nature of the sulphonate groups would attract the water dipoles. If a positively charged surface, such as zirconia, is able to counterbalance the

negative charge on the sulphonate groups, the hydrophilic region of the membrane will be protonated in the presence of both positively and negatively charged species within the polymer framework facilitating the migration of protons through the membrane. In other words, in the absence of fixed counter charges, the long-range coulombic attractive force due to negatively charged sulphonate groups would tend to retain protons within the membrane, even as they are pushed through as a result of the external anode/cathode reactions. If the long-range coulombic attractive force for protons is disrupted by the presence of fixed positively charged surfaces within the polymer network, the protons will move more readily through the membrane. In the Nafion–MZP composite membrane, zirconia is characterised by a relatively high positive surface charge density and zeta potential due to proton adsorption [25]. The high concentration of protons in the electrical double layer is beneficial for the hydrophilicity of Nafion–MZP composite membrane because water species forming the electrical double layer are retained on the MZP surface by the electric field [26]. It is also apparent from the polarisation curves at varying RH values that the performance of PEFCs with Nafion–MZP composite membranes is improved at high load current densities. This could be due to the decreased water flooding that reduces the mass-transfer problem in Nafion–MZP composite membranes. In contrast, at high load current densities, in the PEFCs with pristine Nafion membrane, the water generation rates at the cathode are high enough to substantially affect the effective area of the gas-diffusion layers inside the electrode. In contrast, the high water uptake in Nafion–MZP composite membrane helps hydrating it [27].

In brief, this study demonstrates that Nafion–MZP composite membranes exhibit lower resistance and hence PEFCs with Nafion–MZP composite membranes can sustain higher load current densities, particularly at low RH values, in relation to the pristine Nafion membranes. Hydrated MZP provides better water retention in Nafion–MZP composite membranes than commercial Nafion membrane at reduced RH values. Besides, the impregnation of the MZP into Nafion helps the composite membranes to be less susceptible to high-temperature damage, mitigating their shrinkage at low RH values. The presence of MZP within the membranes apparently obviates the structural changes, and their proton conductivity is retained even at low RH values. Accordingly, the present study provides a novel alternative route to fabricate Nafion–MZP composite membranes with filler particles that absorb water and act as a water reservoir to keep the membrane hydrated even at low RH values that helps the PEFCs to sustain periods of inlet-stream draught without excessive loss in membrane conductivity. Consequently, the auxiliaries desired to humidify the PEFCs could be avoided making the system simpler and hence cost effective.

4 Conclusion

The study describes the synthesis of MZP by a novel co-assembly route and its subsequent impregnation into perfluorosulphonic acid ionomer to form a composite membrane. The porous filler material ameliorates the hydrophilicity of the membrane enhancing its proton conductivity. The combination of robust mesostructure with strong-acid functionality of the composite membrane helps furthering the PEFC performance at low RH values in relation to the PEFC employing pristine Nafion membrane.

Acknowledgement

Financial support from CSIR, New Delhi through a Supra Institutional Project under EFYP is gratefully acknowledged. We thank Professor T. N. Guru Row, Ms. A. Jalajakshi and Dr. Anwar Sahid for the invaluable help.

References

- [1] P. Grant, *Nature* **2003**, 424, 129.
- [2] K. Scott, A. K. Shukla, *Biofuels for Fuel Cells*, (Eds. P. Lens, P. Westermann, M. Haberbauer, A. Moreno), IWA Publishing, London **2005**, pp. 290–294.
- [3] M. K. Song, S. B. Park, Y. T. Kim, K. H. Kim, S. K. Min, H.W. Rhee, *Electrochim. Acta* **2004**, 50, 639.
- [4] S. Panero, P. Fiorenza, M. A. Navarra, J. Romanowska, B. Scrosati, *J. Electrochem. Soc.* **2005**, 152, 2400.
- [5] L. C. Klein, Y. Daiko, M. Aparicio, F. Damay, *Polymer* **2005**, 46, 4504.
- [6] N. Miyake, J. S. Wainright, R. F. Savinell, *J. Electrochem. Soc.* **2001**, 148, A898.
- [7] A. K. Sahu, G. Selvarani, S. Pitchumani, P. Sridhar, A. K. Shukla, *J. Electrochem. Soc.* **2007**, 154, 123.
- [8] A. K. Sahu, G. Selvarani, S. Pitchumani, P. Sridhar, A. K. Shukla, *J. Appl. Electrochem.* **2007**, 37, 913.
- [9] N. H. Jalani, K. Dunn, R. Datta, *Electrochim. Acta* **2005**, 51, 553.
- [10] T. M. Thampan, N. H. Jalani, P. Choi, R. Datta, *J. Electrochem. Soc.* **2005**, 152, 316.
- [11] W. H. J. Hogarth, J. C. D. Costa, J. Drennan, G. Q. Lu, *J. Mater. Chem.* **2005**, 15, 754.
- [12] M. A. Navarra, F. Croce, B. Scrosati, *J. Mater. Chem.* **2007**, 17, 3210.
- [13] Y. Zhai, H. Jhang, J. Hu, B. Yi, *J. Membr. Sci.* **2006**, 280, 148.
- [14] A. K. Sahu, G. Selvarani, S. Pitchumani, P. Sridhar, A. K. Shukla, N. Narayanan, A. Banerjee, N. Chandrakumar, *J. Electrochem. Soc.* **2008**, 155, 686.
- [15] F. Bauer, M. W. Porada, *J. Power Sources* **2005**, 145, 101.
- [16] M. L. Hill, Y. S. Kim, B. R. Einsla, J. E. McGrath, *J. Membr. Sci.* **2006**, 283, 102.
- [17] R. Jiang, H. R. Kunz, J. M. Fenton, *Electrochim. Acta* **2006**, 51, 5596.
- [18] D. T. Boutry, A. D. Geyer, L. Guetaz, O. Diat, G. Gebel, *Macromolecules* **2007**, 40, 8259.
- [19] S. R. Søgaard, Q. Huan, P. Lund, A. Donnadio, M. Casciola, E.M. Skou, *Solid State Ionics* **2007**, 178, 493.
- [20] M. Casciola, G. Alberti, A. Ciarletta, A. Cruccolini, P. Piaggio, M. Pica, *Solid State Ionics* **2005**, 176, 2985.
- [21] P. Krishnan, J. S. Park, T. H. Yang, W. Y. Lee, C. S. Kim, *J. Power Sources* **2006**, 163, 2.
- [22] A. Regina, E. Fontananova, E. Drioli, M. Casciola, M. Sganappa, F. Trotta, *J. Power Sources* **2006**, 160, 139.
- [23] M. H. Woo, O. Kwon, S. H. Choi, M. Z. Hong, H. W. Ha, K. Kim, *Electrochim. Acta* **2006**, 51, 6051.
- [24] V. S. Silva, B. Ruffmann, S. Vetter, A. Mendes, L. M. Madeira, S. P. Nunes, *Catal. Today* **2005**, 104, 205.
- [25] G. Alberti, M. Casciola, U. Constantino, R. Vivani, *Adv. Mater.* **1996**, 8, 291.
- [26] D. Carriere, M. Moreau, K. Lhalil, P. Barboux, J. P. Boilot, *Solid State Ionics* **2003**, 162–163, 185.
- [27] S. P. Nunes, B. Ruffmann, E. Rikowski, S. Vetter, K. Richau, *J. Membr. Sci.* **2002**, 203, 215.
- [28] M. Casciola, D. Bianchi, *Solid State Ionics* **1985**, 17, 287.
- [29] P. Costamagna, C. Yang, A. B. Bocarsly, S. Srinivasan, *Electrochim. Acta* **2002**, 47, 1023.
- [30] W. Grot, C. Ford, G. Rajendran, D. Newark, *US Patent, US 5,919, 583*, **1999**.
- [31] F. Damay, L. C. Klein, *Solid State Ionics* **2003**, 162–163, 261.
- [32] G. Alberti, M. Pica, T. Tarpanelli, PCT patent WO 2005/105667 A1.
- [33] G. Alberti, M. Casciola, M. Pica, T. Tarpanelli, M. Sganappa, *Fuel Cells* **2005**, 5, 366.

- [34] G. Alberti, M. Casciola, D. Capitani, A. Donnadio, R. Narducci, M. Pica, M. Sganappa, *Electrochim. Acta* **2007**, *52*, 8125.
- [35] R. M. Dessau, J. L. Shirker, J. B. Higgins, *Zeolites* **1990**, *10*, 522.
- [36] M. E. Davis, C. Montes, J. Garces, C. Crowder, *Nature* **1988**, *331*, 698.
- [37] M. Estermann, L. B. McCusker, C. Baerlocher, A. Merrouche, H. Kessler, *Nature* **1991**, *352*, 320.
- [38] R. C. Haushalter, L. A. Mundi, *Chem. Mater.* **1992**, *4*, 31.
- [39] M. I. Khan, L. M. Meyer, R. C. Haushalter, A. L. Schweitzer, J. Zubieta, J. L. Dye, *Chem. Mater.* **1996**, *8*, 43.
- [40] J. J. Jimenez, P. M. Torres, P. O. Pastor, E. R. Castellon, A. J. Lopez, D. J. Jones, J. Roziere, *Adv. Mater.* **1998**, *10*, 812.
- [41] E. R. Castellon, J. J. Jimenez, A. J. Lopez, P. M. Torres, J. R. R. Barrado, D. J. Jones, J. Roziere, *Solid State Ionics* **1999**, *125*, 407.
- [42] D. J. Jones, J. Roziere, *Adv. Polym. Sci.* **2008**, *215*, 219.
- [43] A. Sayari, I. Moudrakovski, J. S. reddy, C. I. Ratcliffe, J. A. Ripmeester, K. F. Preston, *Chem. Mater.* **1996**, *8*, 2080.
- [44] B. Tian, X. Liu, B. Tu, C. Yu, J. Fan, L. Wang, S. Xie, G. Stucky, D. Zhao, *Nat. Mater.* **2003**, *2*, 159.
- [45] A. K. Sahu, G. Selvarani, S. D. Bhat, S. Pitchumani, P. Sridhar, A. K. Shukla, N. Narayanan, A. Banerjee, N. Chandrakumar, *J. Membr. Sci.* **2008**, *319*, 298.
- [46] A. Tarafdar, A. B. Panda, N. C. Pradhan, P. Pramanik, *Microporous Mesoporous Mater.* **2006**, *95*, 360.